Journal of Biomechanics 48 (2015) 1300–1309

Contents lists available at ScienceDirect

Journal of Biomechanics

journal homepage: www.elsevier.com/locate/jbiomech
www.JBiomech.com

Hemodynamic transition driven by stent porosity in sidewall aneurysms

Pierre Bouillot [a,b,*], Olivier Brina [a], Rafik Ouared [a], Karl-Olof Lovblad [a], Mohamed Farhat [b], Vitor Mendes Pereira [a,c,d]

[a] Interventional Neuroradiology Unit, Service of Neuroradiology, University Hospital of Geneva, Switzerland
[b] Laboratory for Hydraulic Machines (LMH), École Polytechnique Fédérale de Lausanne (EPFL), Avenue de Cour 33bis, CH-1007 Lausanne, Switzerland
[c] Division of Neuroradiology, Department of Medical Imaging, Toronto Western Hospital, University Health Network, Toronto, ON, Canada
[d] Division of Neurosurgery, Department of Surgery, Toronto Western Hospital, University Health Network, Toronto, ON, Canada

ARTICLE INFO

Article history:
Accepted 15 February 2015

Keywords:
Hemodynamics
Cerebral aneurysm
Stent
Hemodynamic transition
Computational fluid dynamics
Particle imaging velocimetry

ABSTRACT

The healing process of intracranial aneurysms (IAs) treated with flow diverter stents (FDSs) depends on the IA flow modifications and on the epithelization process over the neck. In sidewall IA models with straight parent artery, two main hemodynamic regimes with different flow patterns and IA flow magnitude were broadly observed for unstented and high porosity stented IA on one side, and low porosity stented IA on the other side. The hemodynamic transition between these two regimes is potentially involved in thrombosis formation. In the present study, CFD simulations and multi-time lag (MTL) particle imaging velocimetry (PIV) measurements were combined to investigate the physical nature of this transition. Measurable velocity fields and non-measurable shear stress and pressure fields were assessed experimentally and numerically in the aneurysm volume in the presence of stents with various porosities. The two main regimes observed in both PIV and CFD showed typical flow features of shear and pressure driven regimes. In particular, the waveform of the averaged IA velocities was matching both the shear stress waveform at IA neck or the pressure gradient waveform in parent artery. Moreover, the transition between the two regimes was controlled by stent porosity: a decrease of stent porosity leads to an increase (decrease) of pressure differential (shear stress) through IA neck. Finally, a good PIV–CFD agreement was found except in transitional regimes and low motion eddies due to small mismatch of PIV–CFD running conditions.

1. Introduction

Flow diverter stents (FDSs) are endovascular treatments (Byrne et al., 2010; Pereira et al., 2014b) of sidewall intracranial aneurysms (IAs) (Brisman et al., 2006). These expandable tubular devices made of dense mesh of filaments (Fig. 2) are implanted in the parent artery to cover the IA neck, hence reducing the intra-aneurysmal flow known to promote IA thrombogenesis (Zanaty et al., 2014b; Pereira et al., 2014a). Despite the high success rate of FDS treatments, some complications partly related to hemodynamics issues, e.g. subacute aneurysm rupture, parent artery occlusion or flow persistency, have been reported (Brinjikji et al., 2013; Zanaty et al., 2014a). Recently, hemodynamic indicators measured per-operatively with digital subtracted angiography (DSA) (Pereira et al., 2013a; Chien and Vinuela, 2013) or assessed numerically with computational fluid dynamics (CFD) (Pereira et al., 2014c; Mut et al., 2015; Kulcsar et al., 2012; Zhang et al., 2013) were correlated with successful treatment outcomes. These results highlighted the importance of IA flow modifications in the healing process.

During the last decade, the effect of stent implantation in idealized sidewall IA models with straight parent artery was broadly investigated experimentally (Augsburger et al., 2009; Liou and Li, 2008; Liou et al., 2008; Lieber et al., 2002; Yu and Zhao, 1999; Yu et al., 2012; Bouillot et al., 2014a, 2015) and numerically (Hirabayashi et al., 2006, 2004; Kim et al., 2010; Appanaboyina et al., 2008; Bouillot et al., 2015). Although these studies considered various stent configurations within IAs with different size and shape, identical hemodynamic features were reported regardless of the inflow conditions.

- For unstented and high porosity stented IA, an inflow jet at the distal part of the IA neck driving a large vortex was typically observed in IA.
- When decreasing the stent porosity, the IA flow pattern was strongly altered. In general, a diffuse flow was observed at the IA neck with proximal (distal) inflow (outflow) inverted compared with unstented IA.

* Correspondence to: Hôpitaux universitaires de Genève Service de neuro-diagnostique et neuro-interventionnel, Rue Gabrielle-Perret-Gentil 4, CH - 1211 Genève 14. Tel.: +41 22 372 38 08.
E-mail address: pierre.bouillot@unige.ch (P. Bouillot).

http://dx.doi.org/10.1016/j.jbiomech.2015.02.020
0021-9290/

The transition between these two hemodynamic regimes was controlled by the stent porosity and led to a strong flow reduction potentially involved in thrombosis formation. Indeed, in patient specific IA geometries a similar transition has been predicted with CFD when decreasing the porosity of virtual stent (Shobayashi et al., 2013) and in successfully treated IA with FDS (Zhang et al., 2013). A detailed description of the underlying physics would be therefore very useful for the understanding of thrombosis initiation and design of new devices.

Recently, we proposed in Bouillot et al. (2014a) a possible physical mechanism describing this hemodynamic transition. Our hypothesis schematized in Fig. 1 involved both shear stress and pressure differential at the IA neck difficult to access experimentally. In the present study, we aim to show the evidence of this description supported with quantitative arguments and hence highlight the universal character of the transition. For this purpose, our recent particle imaging velocimetry (PIV) investigations (Bouillot et al., 2014a) were complemented with CFD simulations providing the non-measurable shear stress and pressure fields. These quantities were analyzed in both unstented/stented idealized IA with different porosities and correlated with IA flows measured by PIV and predicted by CFD.

Shear driven: In unstented and high porosity stented IA, the shear stress transmitted at the IA neck, τ_{neck}, induced by the strong velocity gradient in the parent artery, drives a clockwise intra-aneurysmal flow.

Pressure driven: The implantation of low porosity stent impedes the flow at the IA neck resulting in a lower shear stress transmission and an increase of pressure gradient along the parent artery. Consequently, the pressure differentials between the parent artery and the IA, $\Delta p_{\text{prox}} = p_{\text{prox}} - p_{\text{IA}} > 0$ and $\Delta p_{\text{dist}} = p_{\text{dist}} - p_{\text{IA}} < 0$, pushes the circulating fluid inward and outward the IA at the proximal and distal side of the neck, respectively, leading to a counterclockwise flow at the IA neck.

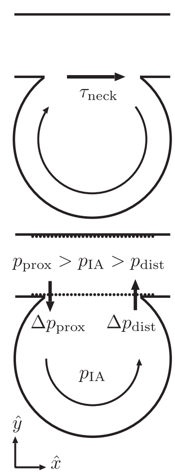

Fig. 1. Schematic representation of the two main flow regimes occurring in stented IA with straight parent artery along with the physical interpretation proposed in Bouillot et al. (2014a). In such a model, the inflow inertia is not directly transmitted to IA. The IA flow is therefore driven by either *shear* stress or *pressure* differential. The transition between these two regimes is driven by the stent porosity.

2. Material and methods

2.1. Experimental and virtual IA models

Fig. 2 shows the idealized sidewall IA geometry considered in the CFD simulations and for the molding of the silicone phantom used in the PIV measurements. In such a model, the stent is expected to expand regularly minimizing the geometry uncertainties in both PIV measurement and CFD simulations. It is composed of a spherical aneurysm of radius $R = 5$ mm located at distance $d_3 = 6$ mm below a straight cylindrical artery of radius $r = 2$ mm. The inlet/outlet length $d_1 = 150$ mm/$d_2 = 110$ mm was set in the silicone model to ensure a fully developed flow in the PIV experiments (van de Vosse and van Dongen, 1998; He and Ku, 1994). Similarly, the CFD simulations were performed with $d_1 = d_2 = 50$ mm minimizing the influence of the boundary conditions on the IA flow.

2.2. Stent properties and virtual deployment

Three commercial of the shelf (COTS) stents showing shear driven (S1), intermediate (S2) and pressure driven (S3) IA hemodynamics in previous PIV study (Bouillot et al., 2014a) were selected for comparison with CFD simulations. Each stent was delivered and implanted in the silicone model following its respective manufacturer guideline (e.g. delivery catheter) in accordance with clinical practice. Their geometrical properties summarized in Table 1 were measured assuming a diamond stent unit cell.

Virtual stents for CFD simulations were modeled by regular meshes made of cylindrical wires of diameter, e, respecting the S1-3 properties in Table 1 and fitting the shape of the parent artery. In order to investigate the hemodynamic transition occurring around S2 porosity, three additional hypothetical stents, S2a–c, with metal coverage proportions $1-\phi = 0.09, 0.15, 0.18$ were also modeled by rescaling the unit cell size, l, of S2. For each stent, two virtual

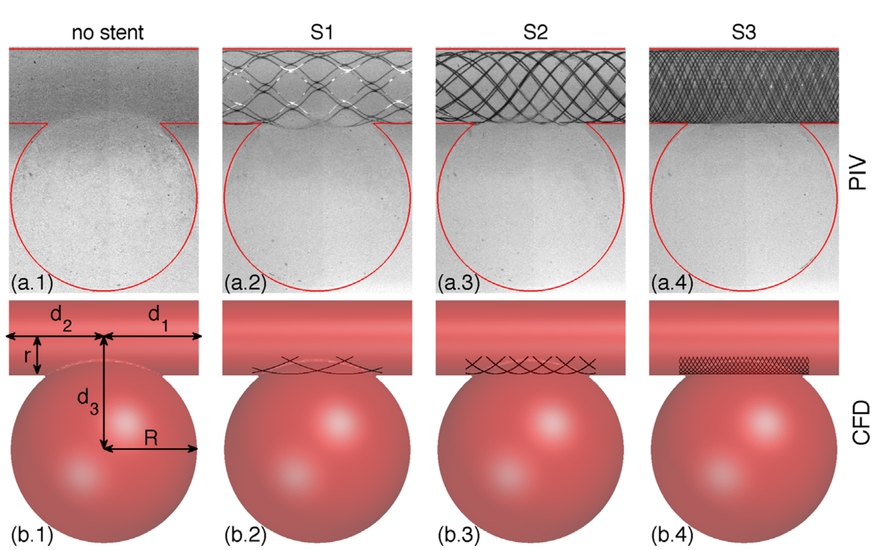

Fig. 2. (columns 1-4) IA model without/with S1, S2 or S3. (row (a)) Picture of the stent implanted in the silicone model filled with the circulating fluid for the PIV measurements. The red lines highlight the limit of the silicone model. (row (b)) Virtual model and stent for the CFD simulations. (For interpretation of the references to color in this figure caption, the reader is referred to the web version of this paper.)